

# Intramyocardial injection of hypoxia-preconditioned adipose-derived stromal cells treats acute myocardial infarction: an in vivo study in swine

Yiyao Jiang · Pengyu Chang · Yu Pei · Baojiang Li ·  
Yongjun Liu · Zhang Zhang · Jing Yu · Delin Zhu ·  
Xiaocheng Liu

Received: 11 December 2013 / Accepted: 23 July 2014 / Published online: 19 August 2014  
© Springer-Verlag Berlin Heidelberg 2014

**Abstract** Hypoxic preconditioning is a promising method for improving the anti-apoptotic and paracrine signaling capabilities of adipose-derived stromal cells (ADSCs). The purpose of this study was to analyze the influence of different hypoxic conditions on ADSCs and the therapeutic effects of hypoxia-preconditioned ADSCs (HPADSCs) on an animal model of myocardial infarction (MI). For the in vitro studies, ADSCs were divided into five groups and cultured in different oxygen concentrations (1, 3, 5, 10, and 21 %). After 24 h, RT-PCR and

western blots showed that 3 % oxygen preconditioning could improve the viability and cytokine secretion of the ADSCs. A Matrigel assay indicated that the HPADSC-conditioned medium could stimulate endothelial cells to form capillary-like tubes. For the in vivo studies, MI was induced by coronary occlusion in 24 mature Chinese minipigs. The animals were divided into three groups and treated by intramyocardial injection with vehicle alone (saline group), with  $1 \times 10^8$  ADSCs cultured in normoxic conditions (ADSCs group) or with  $1 \times 10^8$  ADSCs precultured in 3 % oxygen (HPADSCs group). SPECT and echocardiography demonstrated that cardiac function was improved significantly in the HPADSC transplant group compared with the vehicle control group ( $P < 0.05$ ). Immunofluorescence showed fewer apoptotic cells and more small- to medium-sized vessels in the HPADSC transplantation group ( $P < 0.05$ ). Three percent oxygen is the optimum preconditioning treatment for ADSCs. HPADSC transplantation can prevent ventricular remodeling and reduce the infarct size.

Y. Jiang · Y. Pei · Y. Liu · D. Zhu · X. Liu  
Department of Cardiovascular Surgery, TEDA International  
Cardiovascular Hospital Cardiovascular Clinical Hospital of Tianjin  
Medical University, 61# Third Avenue Tianjin Economic  
Development Area, Tianjin 300457, China

P. Chang  
Department of Radiation Oncology in the First Bethune Hospital of  
Jilin University Changchun, Jilin 130021, China

Y. Pei · X. Liu (✉)  
Peking Union Medical College, Chinese Academy of Medical  
Sciences, Beijing 100730, China  
e-mail: xcliu0727@sina.com

B. Li  
Department of Pathology, the Fifth Central Hospital of Tianjin,  
Tianjin 300450, China

Y. Liu · D. Zhu (✉)  
Alliancells Biosciences Co., Ltd, 45 Dongjiu Road, Airport  
Economic Area, Tianjin 300304, China  
e-mail: delzhu@126.com

Z. Zhang  
Department of Radiology, Tianjin Medical University General  
Hospital, Tianjin 300052, China

J. Yu  
Department of Radiology, Tianjin First Center Hospital,  
Tianjin 300192, China

**Keywords** Hypoxia-preconditioned · Myocardial infarction ·  
ADSCs · Angiogenesis · Transplantation

## Introduction

Myocardial infarction (MI) remains a widespread and important cause of morbidity and mortality across the world (Reddy 2004; Lopez et al. 2006). Although advanced therapies have improved short-term survival following MI, the remodeling process caused by cardiomyocyte loss and the limited endogenous repair mechanism ultimately lead to progressive heart failure (Fraccarollo et al. 2012). Several animal experiments have demonstrated that the cardiac function of MI could be improved by stem cell transplantation (Fuchs et al. 2001). In

the clinic, cell-based therapy is a promising option to treat MI. Compared with other stem cells, adipose-derived stromal cells (ADSCs), which are easily obtained in abundant amounts, may have enormous therapeutic potential to reduce myocardial cell apoptosis, limit infarct size and restore myocardial perfusion (Mazo et al. 2011; Panfilov et al. 2013; Houtgraaf et al. 2012). However, the response of acute myocardial infarction (AMI) to treatment is dependent on the residence time of the ADSCs in the infarct zone because few transplanted stem cells can survive more than 2 weeks in the infarct microenvironment (Freyman et al. 2006). Therefore, it is necessary to find a more efficient and convenient way to improve the anti-apoptotic capability of implanted ADSCs.

Recently, some studies have shown that the proliferation, migration and anti-apoptotic abilities of ADSCs are enhanced when the cells are cultured under hypoxic conditions. ADSCs were preconditioned for 24 h with hypoxia and then exposed to simulated ischemia for another 24 h. Hypoxic preconditioning significantly increased the viability of the ADSCs and reduced cell injury and apoptosis compared with non-preconditioned cells under ischemic conditions (Stubbs et al. 2012; Kim et al. 2011, 2012). In addition, Lavrentieva et al. (2010) found that umbilical cord-derived human mesenchymal stem cells adapted their energy consumption and metabolism according to an appropriate hypoxic environment. However, the optimal oxygen concentration to improve the performance of ADSCs is still under investigation. Therefore, the purpose of the current study was to investigate whether HPADSCs display higher anti-apoptotic capacity and whether intramyocardial transplantation of HPADSCs improves cardiac function in the infarcted heart through a paracrine effect.

## Materials and methods

### Human ADSC preparation

Adipose tissue samples were obtained from the subcutaneous fat of eight adult Chinese female donors (average age =  $24.2 \pm 3.4$ ) with informed written consent. ADSCs were isolated, cultured and prepared as previously described (Qu et al. 2013). The ADSCs were characterized by cell surface markers using flow cytometry with antibodies against CD34, CD45, CD71, CD73, CD90, CD105 and HLA-DR.

### Hypoxic preconditioning

The ADSCs were cultured in a hypoxia chamber incubator (Forma Water Jacketed CO<sub>2</sub> Incubator; Thermo Fisher Scientific) at 37 °C in 5 % CO<sub>2</sub> and various oxygen concentrations (1, 3, 5, and 10 %) with a balance of N<sub>2</sub> for 24 h. These ADSCs were designated as hypoxia-preconditioned

ADSCs. Normoxia-preconditioned ADSCs (for 24 h in 95 % air, 5 % CO<sub>2</sub>) were used as the control.

### Quantitative RT-PCR (qPCR)

To analyze the mRNA levels of VEGF-A, HGF, PLGF, HIF-1 $\alpha$ , Bax, Bcl-2 and BNip3 in each group, total mRNA was isolated from human ADSCs using the PureLink™ RNA Mini Kit (Life Technologies). Subsequently, the mRNA was reverse-transcribed using TaqMan Reverse Transcription Reagents (Applied Biosystems). Quantitative real-time reverse transcription–polymerase chain reactions (RT-qPCR) were performed using an ABI PRISM 7500 Sequence Detection System and the primers listed in Table 1. The fold changes of expression of each target mRNA relative to  $\beta$ -actin under experimental conditions compared with the control conditions were calculated based on the threshold cycle ( $C_T$ ) as follows:  $r = 2^{-\Delta(\Delta C_T)}$ , where  $\Delta C_T = C_T$  (target) -  $C_T$  ( $\beta$ -actin) and  $\Delta(\Delta C_T) = \Delta C_T$  (experimental) -  $\Delta C_T$  (control).

### Western blot

The cells were lysed with RIPA buffer (Sigma-Aldrich, USA) and the protein concentrations were determined using the BCA Protein Assay Reagent (Pierce Biotechnology). Total protein (30  $\mu$ g) was separated electrophoretically, transferred to a PVDF membrane and probed using monoclonal primary antibodies against Bax (1:500), Bcl-2 (1:500), HIF-1 $\alpha$  (1:500),  $\beta$ -actin (1:500) (all from Abcam, UK) and BNip3 (1:500; Santa Cruz, USA) followed by an HRP-conjugated secondary antibody (1:1000; Abbiotec, USA). Bands were revealed using an ECL kit (Bio-Rad, USA) and analyzed using Image-Pro Plus software.

### Matrigel morphogenesis assay

The effect of HPADSC-conditioned medium on the in vitro formation of capillary-like tubes on Matrigel was evaluated. The assay was performed as described (Efimenko et al. 2011), with some modifications. Briefly, conditioned medium was collected from ADSCs cultured in hypoxic and standard conditions. Matrigel (200  $\mu$ l; BD Bioscience) was polymerized on 24-well plates. Human umbilical vein endothelial cells were suspended in conditioned medium and seeded on the top of the matrigel at a concentration of  $2 \times 10^4$  cells per well. After 24 h of incubation at 37 °C, the formation of capillary-like structures was assayed under a light microscope, and the images were analyzed using Image-Pro software.

**Table 1** The primer sequences and the amplification product sizes of the target genes

Genes	Primer nucleotide sequence	Product size (bp)
VEGF-A	Forward:5'-GAAAGACAAATCACAGTTCCG-3' Reverse:5'-ATGTGTCTCTCTCTTCGCCG-3'	232
HGF	Forward:5'- ACCCTGGTGTTCACAAGCA -3' Reverse:5'- GCAAGAATTTGTGCCGGTGT-3'	181
PLGF	Forward:5'- AGTCCTGTCCAAAAGTAGGG-3' Reverse:5'- AGTGTGAGGGGAGATCACGG -3'	195
HIF-1 $\alpha$	Forward:5'-TCCATGTGACCATGAGGAAA-3' Reverse:5'-CCAAGCAGGTCATAGGTGGT-3'	251
Bax	Forward:5'-ACCAAGAAGCTGAGCGAGTGT-3' Reverse:5'-ACAAACATGGTCACGGTCTGC-3'	462
Bcl-2	Forward:5'- AGATGTCCAGCCAGCTGCAC-3' Reverse:5'-GTTGACTTCACTTGTGGCC-3'	387
BNip3	Forward:5'-TTTAAACACCCGAAGCGCAC-3' Reverse:5'-ACGAAGGCCAGGATCTAAC-3'	270
$\beta$ -actin	Forward:5'-GAAGGTGACAGCAGTCGGTT-3' Reverse:5'-GGGACTTCTGTAAACAACGCAT-3'	127

### Animal experiments

Adult Chinese minipigs (20.2 $\pm$ 2.7 kg; Tianjin, China) were used in this study. The swine were immunosuppressed by daily administration of cyclosporin A (Kim et al. 2005). All procedures were approved by the Institutional Animal Care and Use Committee of the TEDA International Cardiovascular Hospital and were performed according to the guidelines published in the Recommendations from the Declaration of Helsinki.

### Surgical model of myocardial infarction

A model of myocardial infarction was established in Chinese minipigs by the same surgeon under the conditions described previously (Lin et al. 2010). The pigs were sedated and anesthetized with an intramuscular injection of ketamine hydrochloride (20 mg/kg) and xylazine hydrochloride (2 mg/kg). After intravenous injection of thiopental sodium (10 mg/kg) and vecuronium bromide (0.1 mg/kg), the pigs were intubated and mechanically ventilated with 0.5 % enflurane at the time of surgery. Under continuous electrocardiographic monitoring and oxygen saturation, a median sternotomy was performed. After entering the pericardial space, the mid-third of the left anterior descending (LAD) artery was ligated with 5–0 polypropylene after two 3-min intermittent brief preconditioning occlusions. A bolus dose of lignocaine was given intravenously (1 mg/kg) and was maintained at 1 mg/min kg by an intravenous drip. The MI was confirmed by the elevation of the ST segment of the ECG. The animals were randomized into control, ADSCs and HPADSCs groups ( $n=8$  each). The infarct border region was visually identified and either  $1 \times 10^8$  cells/2 ml or saline solution was injected with a syringe in 10

locations within 10 minutes. During the 3 days following the surgery, the pigs received intramuscular penicillin at 2.4 million U/day. The principle surgeon prepared the model, and the injections were blinded to the treatment groups.

### Echocardiography

The cardiac function was evaluated by echocardiography (Vivid E9; GE) immediately after the surgery and 6 weeks later using a 3.5-MHz annular array transducer. After anesthesia, parasternal long-axis views were obtained with both M-mode and 2D echo images. The left ventricular end-diastolic diameter (LVEDD) and end-systolic diameter (LVESD) were measured perpendicular to the long axis of the ventricle at the location of the papillary muscle insertion site. The left ventricle ejection fraction (LVEF) was calculated automatically by the echocardiography system as  $(LVEDV - LVESV) / LVEDV \times 100 \%$ , where LVEDV is the left ventricular end diastolic volume calculated as  $7.0 \times LVEDD^3 / (2.4 + LVEDD)$  and LVESV is the left ventricle end systolic volume calculated as  $7.0 \times LVESD^3 / (2.4 + LVESD)$ .

### Technetium 99 m-sestamibi single photon emission tomography

A technetium-99m sestamibi single photon emission tomography (99mTc-SPECT MIBI; GE) measurement was performed at the same time as the echocardiography. A 0.4-mCi per kg dose of 99mTc sestamibi was injected intravenously 30 min before the ECG-gated 99mTc-SPECT MIBI scan. The SPECT was performed using a circular 180 $^\circ$  acquisition for 60 projections at 20 s per projection. Perfusion defects were

calculated using a scintigraphic bull's eye technique, and the LVEF was assessed with an automatic program.

#### Histological assessments

After completion of all the measurements, the hearts were arrested with potassium chloride and rapidly excised. Cross-sectional areas of the ventricular muscle, scar area, and scar thickness were measured with computed planimetry. A cube of tissue (5 mm) from the peri-infarct zone was embedded in paraffin and cut into 10- $\mu$ m sections.

#### Hematoxylin and eosin staining

After drying, the slices were immersed in distilled water for 1 min prior to dehydration in a gradient ethanol solution. Then, they were put into a hematoxylin solution for 15 s, washed with distilled water, immersed in Scott solution for 10 s, and washed again with distilled water. After being immersed in eosin solution for 10 s, these heart slices were dehydrated again in a gradient ethanol solution, treated with dimethylbenzene and covered with coverslips. The slices were evaluated under a light microscope and quantified at  $\times 400$  magnification.

#### Masson trichrome staining

To estimate the degree of fibrosis, the slides were dewaxed, rehydrated and stained in Celestin blue-hematoxylin before differentiating in 1 % acid alcohol. The sections were washed in tap water and stained in an acid fuchsin solution for 5 min. The slides were rinsed in distilled water before being treated with a phosphomolybdic acid solution for 5 min. Subsequently, the sections were counterstained in aniline blue for 10 min, rinsed in distilled water, and treated with 1 % acetic acid for 2 min. Finally, the sections were dehydrated in graded alcohol, cleared in xylene, and mounted. The sections were viewed under a light microscope. The fibrosis areas were analyzed by Image Pro Plus software.

#### Immunohistochemistry

Sections of the peri-infarction tissue were selected to quantify the inflammatory cells and capillary density by immunohistochemistry using CD4 and vWF, respectively. The sections were washed in PBS and incubated separately overnight with the following primary antibodies: mouse anti-CD4 and mouse anti-vWF. After incubation, the sections were washed in PBS and incubated in the vectastain avidin-biotin complex (ABC) kit for 1.5 h. The slides were then washed and mounted for light microscopy. The inflammatory cells and capillary density were analyzed using the Image Pro Plus software.

#### Immunofluorescent staining

Serial cutting sections were used for immunofluorescent staining. Formalin-fixed, paraffin-embedded tissue sections were serially rehydrated in 100, 95, and 70 % ethanol after deparaffinization with xylene. The antigen retrieval procedures were then performed. The slides were microwaved in 10 mmol/L citrate buffer (pH=6.0) for 3 min. After 30 min of cooling, the slides were washed in PBS 3 times for 5 min each. The tissue sections were incubated in a blocking solution containing 10 % goat serum and 1 % bovine serum albumin in PBS to reduce nonspecific binding. The sections were incubated with isolectin B4 (1:200; Santa Cruz), Ki67 (1:200; Santa Cruz) and anti-beta 2 human microglobulin (1:200; Abcam) overnight at 4 °C. The sections were then incubated for 1 h at room temperature with an Alexa Fluor 488 donkey anti-rabbit immunoglobulin G or an Alexa Fluor 594 donkey anti-mouse immunoglobulin G. The nuclei were counterstained with DAPI (2.5  $\mu$ g/ml in PBS; Molecular Probes). The slides were visualized using a Leica TCS SP5 confocal microscope.

#### TUNEL assay

Cell apoptosis was detected by a terminal deoxynucleotidyl transferase-mediated dUTP-biotin nick end labeling (TUNEL) assay using the In Situ Cell Death Detection Kit, Fluorescein according to the manufacturer's instructions (Roche). The TUNEL-positive nuclei were counted from five random fields near the area of infarction on each section.

#### Statistical analysis

All the data were analyzed using SPSS 17.0. The data are reported as means $\pm$ SEM. For the analysis of differences between two groups, a Student's *t* test was performed. For multiple groups, one-way ANOVA was used to analyze the significance of the differences between the mean values of the experimental and the control groups. Probability values (*P*) less than 0.05 were considered significant.

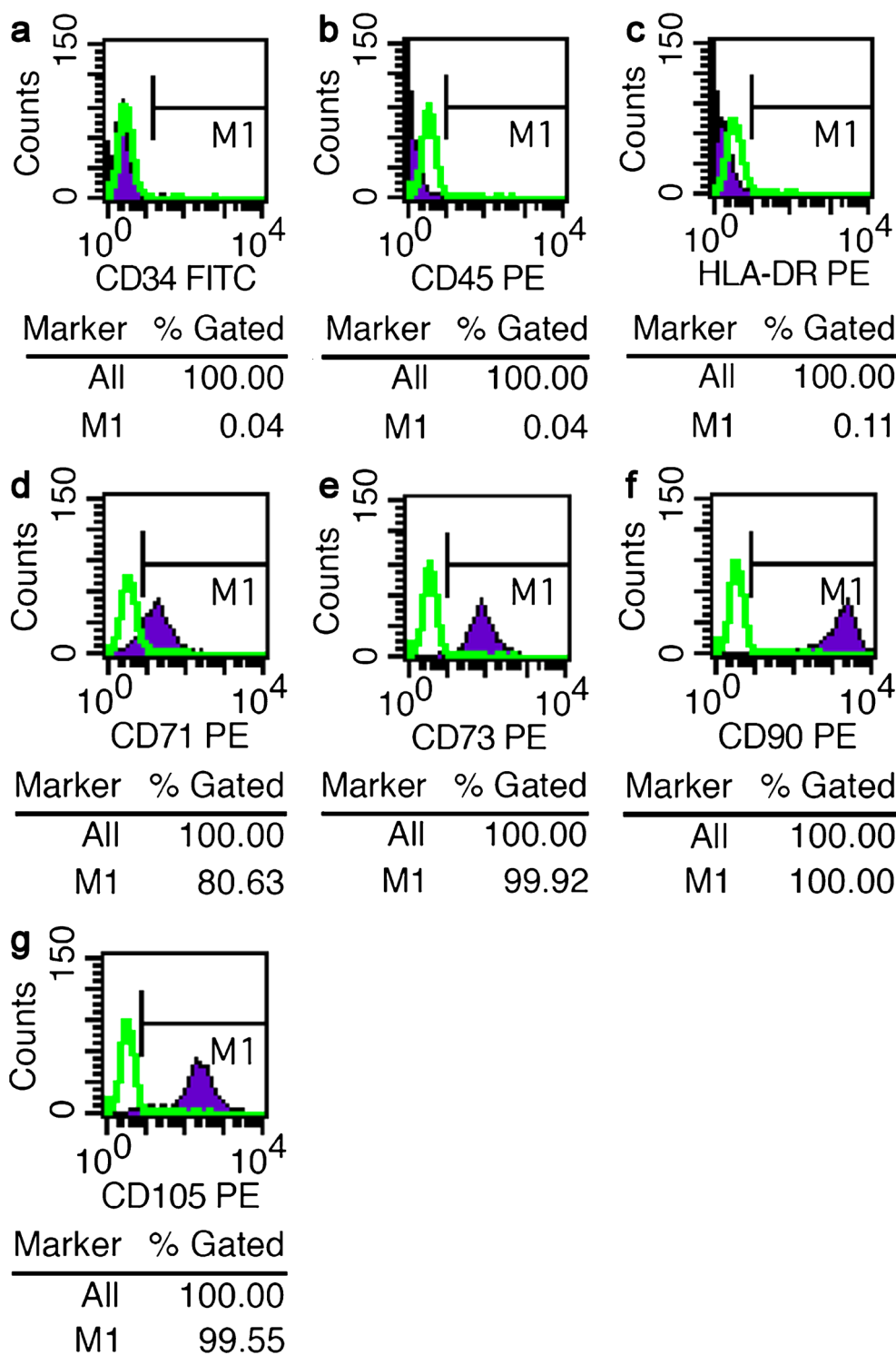
## Results

#### Characterization of human ADSCs

Cultured ADSCs at four to six passages were used in this study. Flow cytometry demonstrated that these cells were negative for CD34, CD45 and HLA-DR and positive for CD71, CD73, CD90 and CD105 (Fig. 1a-g). These results indicated that these cells maintained a typical ADSC phenotype, as previously reported (Yang et al. 2013).



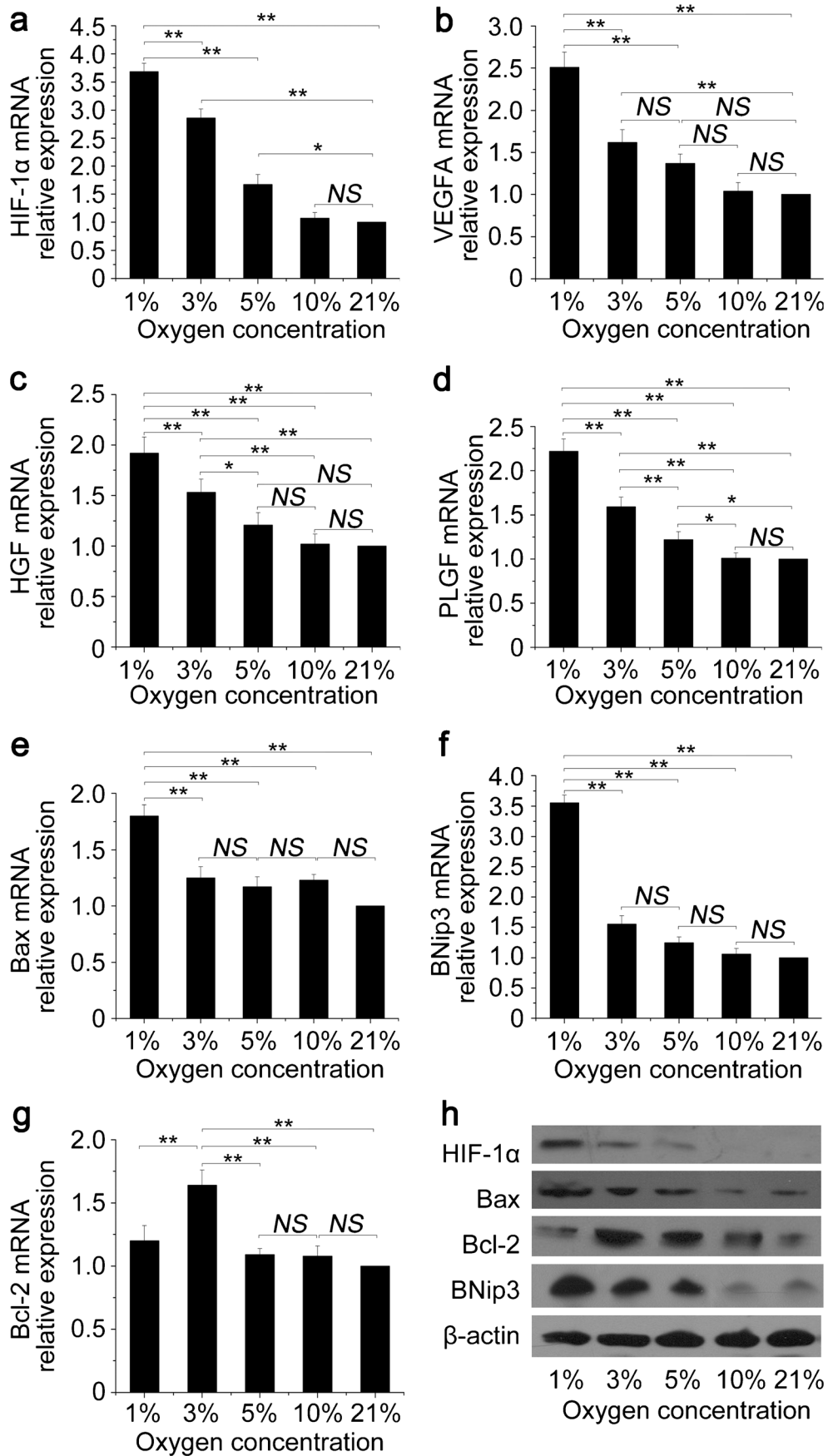
**Fig. 1** The phenotypic characterization of the hADSCs by flow cytometry (a–g)



**Hypoxia affects mRNA and protein expression in ADSCs**

We examined the mRNA expression of angiogenesis- and apoptosis-related genes by RT-qPCR in cells cultured under hypoxic (1, 3, 5, and 10 % oxygen) and normoxic (21 % oxygen) conditions for 24 h. HIF-1 $\alpha$  is recognized as a key modulator of the transcriptional response to hypoxic stress.

The level of HIF-1 $\alpha$  expression was gradually and significantly upregulated as the oxygen concentration in the cell culture was reduced, and the highest expression was found when cells were cultured under 1 % oxygen ( $3.68 \pm 0.15$  in the 1 % group compared with  $2.86 \pm 0.16$  in the 3 % group,  $P=0.009$ , and  $1.67 \pm 0.18$  in the 5 % group,  $P=0.001$ ). In addition, when compared with the HIF-1 $\alpha$  mRNA levels in cells



◀ **Fig. 2** mRNA expression of HIF-1 $\alpha$ , VEGF-A, HGF, PLGF, Bax, Bcl-2 and BNip3 in ADSCs after culturing in different oxygen concentrations (1, 3, 5, 10, and 21 %) for 24 hours. **a** The level of HIF-1 $\alpha$  expression was gradually and significantly upregulated with the decrease of oxygen concentration. **b** Compared with the control group, the level of VEGF-A expression was significantly higher in the cells cultured under 1 and 3 % oxygen. **c** The level of HGF expression was highest in the cells cultured under 1 % oxygen. **d** The fold change of PLGF mRNA expression was similar to that of HGF; it was the highest under 1 % oxygen. **e** The fold change of Bax mRNA expression was the highest under 1 % oxygen. **f** The level of BNip3 expression was significantly higher under 1 % oxygen than under any other concentration. **g** The fold change of Bcl-2 mRNA expression was highest under 3 % oxygen. **h** Western blotting results of HIF-1 $\alpha$ , Bax, Bcl-2 and BNip3 protein expression in ADSCs cultured in different oxygen concentrations for 24 h. Beta-actin was used as the reference gene. ( $n=6$  per group; \* $P<0.05$ , \*\* $P<0.001$ , NS not significant)

cultured under 21 % oxygen, there were significant differences in cells cultured under 3 and 5 % oxygen ( $P=0.000$  and  $P=0.01$ , respectively), while there was no significant difference between the 10 and 21 % oxygen groups (Fig. 2a).

The level of VEGF-A expression was significantly higher in cells cultured under 1 and 3 % oxygen compared with cells cultured under normoxic conditions ( $P=0.001$  and  $P=0.009$ , respectively). The cells cultured under 1 % oxygen showed the highest expression level ( $2.51\pm 0.18$  in the 1 % group compared with  $1.62\pm 0.15$  in the 3 % group,  $P=0.001$ , and  $1.37\pm 0.11$  in the 5 % group,  $P=0.001$ ; Fig. 2b).

The level of HGF expression was significantly higher in cells cultured under 1 and 3 % oxygen when compared with cells cultured under normoxic conditions ( $P=0.000$  and  $P=0.001$ , respectively). The cells cultured under 1 % oxygen showed the highest expression level ( $1.92\pm 0.16$  in the 1 % group compared with  $1.53\pm 0.13$  in the 3 % group,  $P=0.003$ , and  $1.21\pm 0.12$  in the 5 % group,  $P=0.000$ ; Fig. 2c).

PLGF expression was similar to that of VEGF-A and HGF; the cells cultured under 1 % oxygen showed the highest expression level ( $2.22\pm 0.14$  in the 1 % group compared with  $1.59\pm 0.11$  in the 3 % group,  $P=0.000$ , and  $1.22\pm 0.09$  in the 5 % group,  $P=0.000$ ; Fig. 2d).

The fold change of the Bax mRNA expression was highest under 1 % oxygen compared with the other groups ( $1.8\pm 0.1$  in the 1 % group compared with  $1.25\pm 0.1$  in the 3 % group,  $P=0.006$ ,  $1.17\pm 0.09$  in the 5 % group,  $P=0.002$ , and  $1.23\pm 0.05$  in the 10 % group,  $P=0.005$ ). There was no significant difference between Bax mRNA expression under 3, 5, or 10 % oxygen compared with the control group ( $P>0.05$ ; Fig. 2e).

The overexpression of BNip3 is related to mitochondrial defects and cell death during hypoxia. The level of BNip3 expression was significantly higher under 1 % oxygen ( $3.55\pm 0.13$  under 1 % oxygen compared with  $1.55\pm 0.14$  under 3 % oxygen,  $P=0.000$ ,  $1.24\pm 0.1$  under 5 % oxygen,  $P=0.000$ , and  $1.06\pm 0.09$  under 10 % oxygen,  $P=0.000$ ). There were no

significant differences among the 3, 5, 10, and 21 % oxygen groups (Fig. 2f).

Interestingly, the fold change of Bcl-2 mRNA expression was highest under 3 % oxygen ( $1.64\pm 0.12$  under 3 % oxygen compared with  $1.2\pm 0.12$  under 1 % oxygen,  $P=0.008$ ,  $1.09\pm 0.05$  under 5 % oxygen,  $P=0.002$ , and  $1.08\pm 0.08$  under 10 % oxygen,  $P=0.001$ ); there were no significant differences among the 1, 5, 10, and 21 % oxygen groups (Fig. 2g).

Western blotting was used to analyze the effect of hypoxic preconditioning on protein expression in ADSCs. The highest protein levels of HIF-1 $\alpha$ , Bax and BNip3 were found when the cells were cultured under 1 % oxygen, whereas the Bcl-2 protein expression was the highest under 3 % oxygen (Fig. 2h).

HPADSC-conditioned medium stimulates capillary-like tube formation in ECs

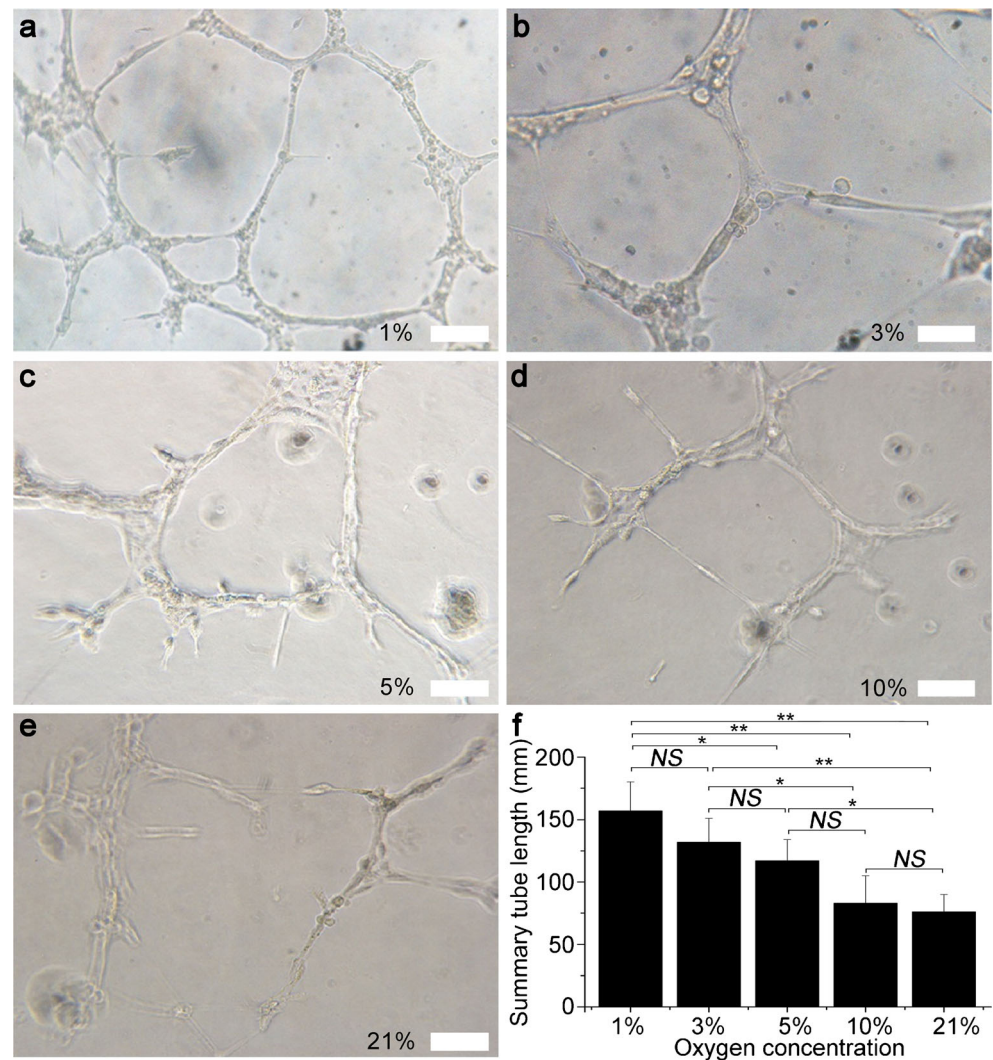
Conditioned medium from cells cultured under different oxygen concentrations affects capillary-like tube formation (Fig. 3a–e). Conditioned medium from cells cultured under hypoxia stimulated the formation of capillary-like structures on Matrigel to a greater extent than cells cultured under normoxic conditions. This observation was especially significant for cells grown under 1 % oxygen ( $P=0.000$ ), while the difference between the 3 and 5 % oxygen groups was insignificant ( $P=0.363$ ; Fig. 3f).

Cardiac Function

The animal model of AMI was injected with either  $1\times 10^8$  ADSC,  $1\times 10^8$  HPADSC or saline. All of the echocardiograph and SPECT measurements for the control, ADSCs and HPADSCs groups were compared with baseline measurements from the AMI model prior to surgery.

Echocardiography shows that the ejection fraction decreased in the control, ADSC and HPADSC groups ( $74.4\pm 4.56$  compared with  $72.12\pm 5.92$  %,  $72.00\pm 3.58$  compared with  $71.41\pm 5.39$  % and  $76.2\pm 3.96$  compared with  $73.57\pm 4.38$  %, respectively); however, there were no significant differences (Fig. 4a). The wall thickening rate was increased from  $16.7\pm 4.79$  to  $19.7\pm 6.27$  % in the control group, whereas it decreased in the HPADSC transplant group from  $18.1\pm 5.28$  to  $13.53\pm 4.79$  %; however, this difference was not significant ( $P=0.087$ ; Fig. 4b). The LVEDV decreased significantly in the HPADSC transplant group after the transplantation treatment ( $69.87\pm 5.98$  compared with  $50.42\pm 10.1$  ml,  $P=0.012$ ; Fig. 4c). The LVESV was also significantly improved after transplantation ( $18.17\pm 3.78$  compared with  $12.8\pm 3.42$  ml,  $P=0.027$ ; Fig. 4d). Although the LVEDV and LVESV were improved in the ADSC transplant group, there were no significant differences.

**Fig. 3** Capillary-like tube formation in the presence of conditioned medium from HPADSCs. Morphology of the tubes formed by human umbilical vein endothelial cells on Matrigel that were incubated with conditioned medium from ADSCs preconditioned in different oxygen concentrations (a–e). The average lengths of the formed tubes were measured (f). (\* $P < 0.05$ , \*\* $P < 0.001$ , NS not significant). Bar 100  $\mu\text{m}$



The ejection fraction and myocardial infarct size were evaluated by a  $^{99\text{m}}\text{Tc}$ -SPECT MIBI scan (Fig. 4e–j). Six weeks after cell transplantation, the cardiac ejection fraction in the HPADSC transplant group was increased ( $63.3 \pm 5.86$  compared with  $74.0 \pm 6.56$  %,  $P = 0.104$ ), whereas it was decreased in the control and ADSC transplant groups ( $67.1 \pm 4.73$  compared with  $63.33 \pm 7.02$  %,  $P = 0.193$ , and  $73.2 \pm 4.36$  compared with  $70.37 \pm 5.65$  %,  $P = 0.366$ , respectively). However, none of these differences in cardiac ejection fraction were significant (Fig. 4k). The myocardial infarction area in the ADSCs and HPADSCs was significantly better after cell transplantation ( $34.67 \pm 7.51$  compared with  $27.53 \pm 3.21$  %,  $P = 0.036$ , and  $31.67 \pm 9.07$  compared with  $17.76 \pm 5.03$  %,  $P = 0.037$ , respectively; Fig. 4l).

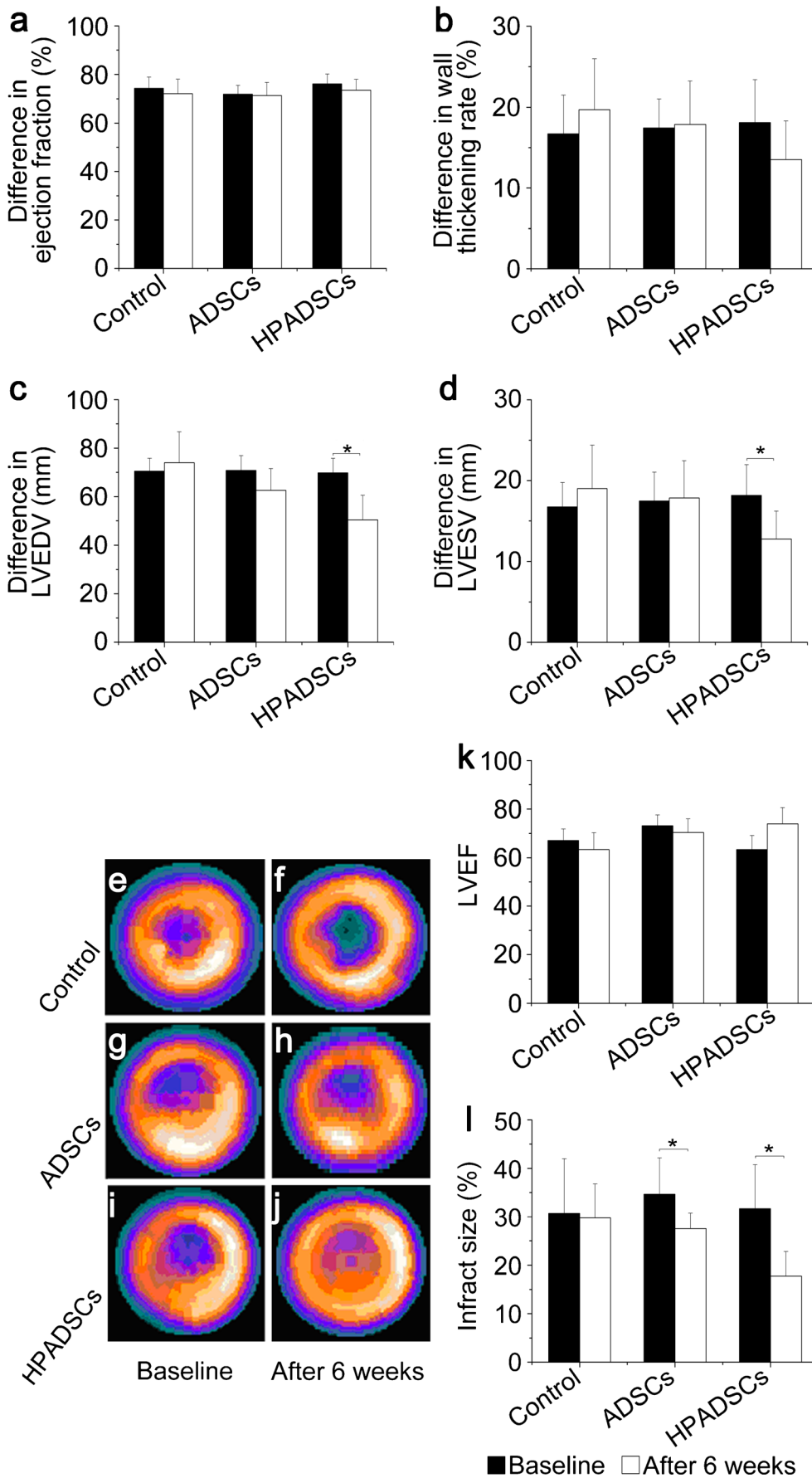
#### Histological studies

Myocardial tissues from the infarct regions in the three groups were evaluated by H&E, Masson's Trichrome staining,

immunohistochemistry and immunofluorescence staining. H&E and Masson's Trichrome staining showed that severe fibrosis occurred in the control group at 6 weeks after the AMI. Although there was little fibrous repair, there was more inflammatory cell infiltration in the ADSC and HPADSC transplantation groups (Fig. 5a–f). Consistent with the H&E findings, the Masson's Trichrome staining showed that the injection of ADSCs or HPADSCs reduced fibrosis in the

**Fig. 4** Echocardiographic and SPECT assessment of cardiac function after 6 weeks. There was no statistically significance difference in the Ejection Fraction (EFs) or wall thickening rates (a, b). Compared with the control group, LVEDV and LVESV decreased in the HPADSC transplantation group (c, d). The EFs and infarct sizes were evaluated by SPECT (e–j). There were no differences in the EFs among the different groups (k). Infarct size reduced in both the ADSC and HPADSC transplantation groups. In the HPADSC transplantation group, the smaller infarct size was more obvious (l). ( $n = 8$  per group; \* $P < 0.05$ )





infarcted hearts. In the ADSC transplant group, the fibrosis area was decreased when compared with the control group; however, the difference was not significant ( $46.27 \pm 9.67$  compared with  $53.21 \pm 12.79$  %,  $P=0.426$ ). In the HPADSC transplant group, the fibrosis area was better than in the control group ( $31.57 \pm 6.37$  compared with  $53.21 \pm 12.79$  %,  $P=0.037$ ). Although there was no significant difference between the ADSC transplant group and the HPADSC transplant group, the trend of a decreasing fibrosis area in the HPADSC transplant group was obvious (Fig. 5g).

Immunohistochemistry staining with CD4 and vWF were used to quantify the inflammatory cells and capillary density (Fig. 6a–f). An antibody against CD4 demonstrated an increase in the amount of inflammatory cells in the peri-infarct zone in the HPADSC and ADSC groups; the difference between the HPADSC group and the control group was

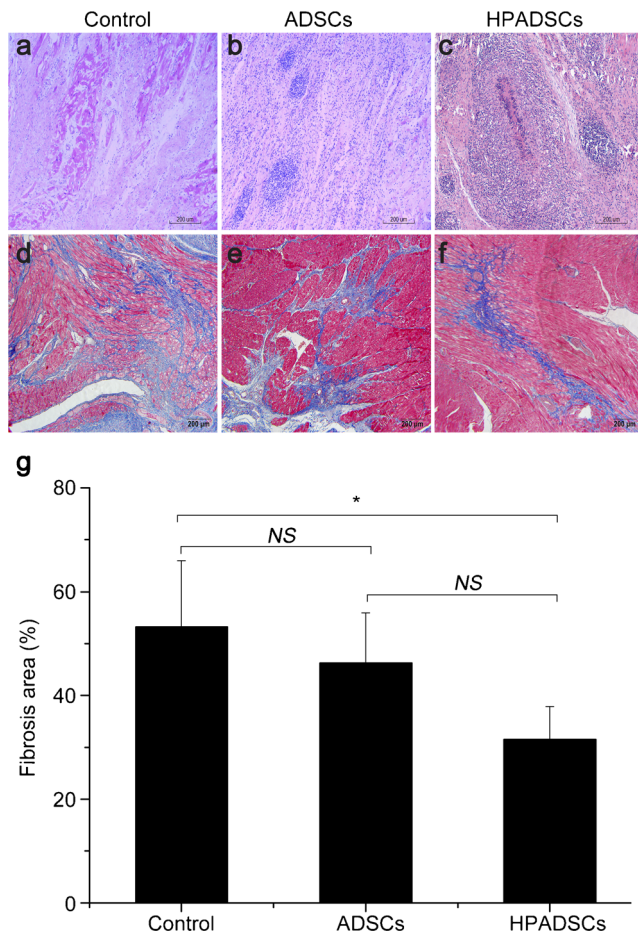


**Fig. 5** Fibrosis and inflammatory cell infiltration occurred in the ADSC and HPADSC transplantation groups; however, only fibrosis was observed in the control group at 6 weeks after AMI (a–f). Severe fibrosis in the control group. The collagen content was reduced in the ADSC and HPADSC transplantation groups, especially in the HPADSC group (g). Bar 200  $\mu$ m

significant ( $39.4 \pm 13.5$  compared with  $12.7 \pm 4.3$ /Field, respectively,  $P=0.02$ ; Fig. 6g). The capillary densities were analyzed in the transplantation and control groups using an antibody against vWF; the total number of blood vessels in the HPADSC group was greater than that in the control group. The difference between the HPADSC and ADSC groups was statistically significant ( $15.4 \pm 3.7$  compared with  $22.6 \pm 4.6$  vessels/ $0.2 \text{ mm}^2$ , respectively,  $P=0.04$ ; Fig. 6h).

To determine whether ADSCs could promote angiogenesis, engraft and proliferate surrounding the myocardial

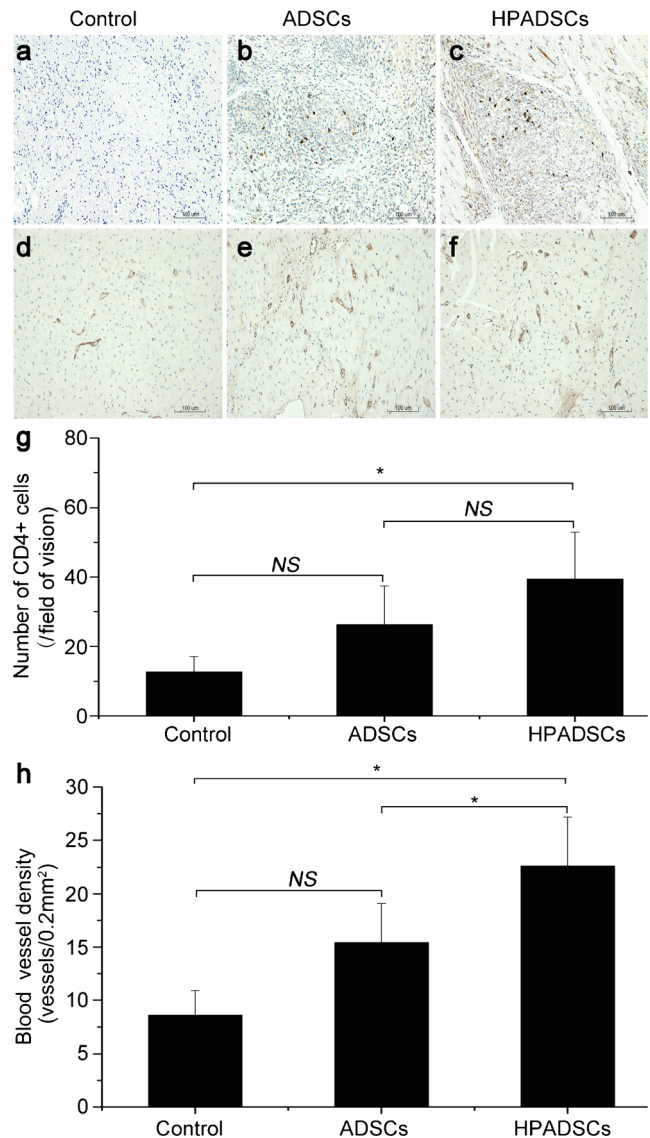
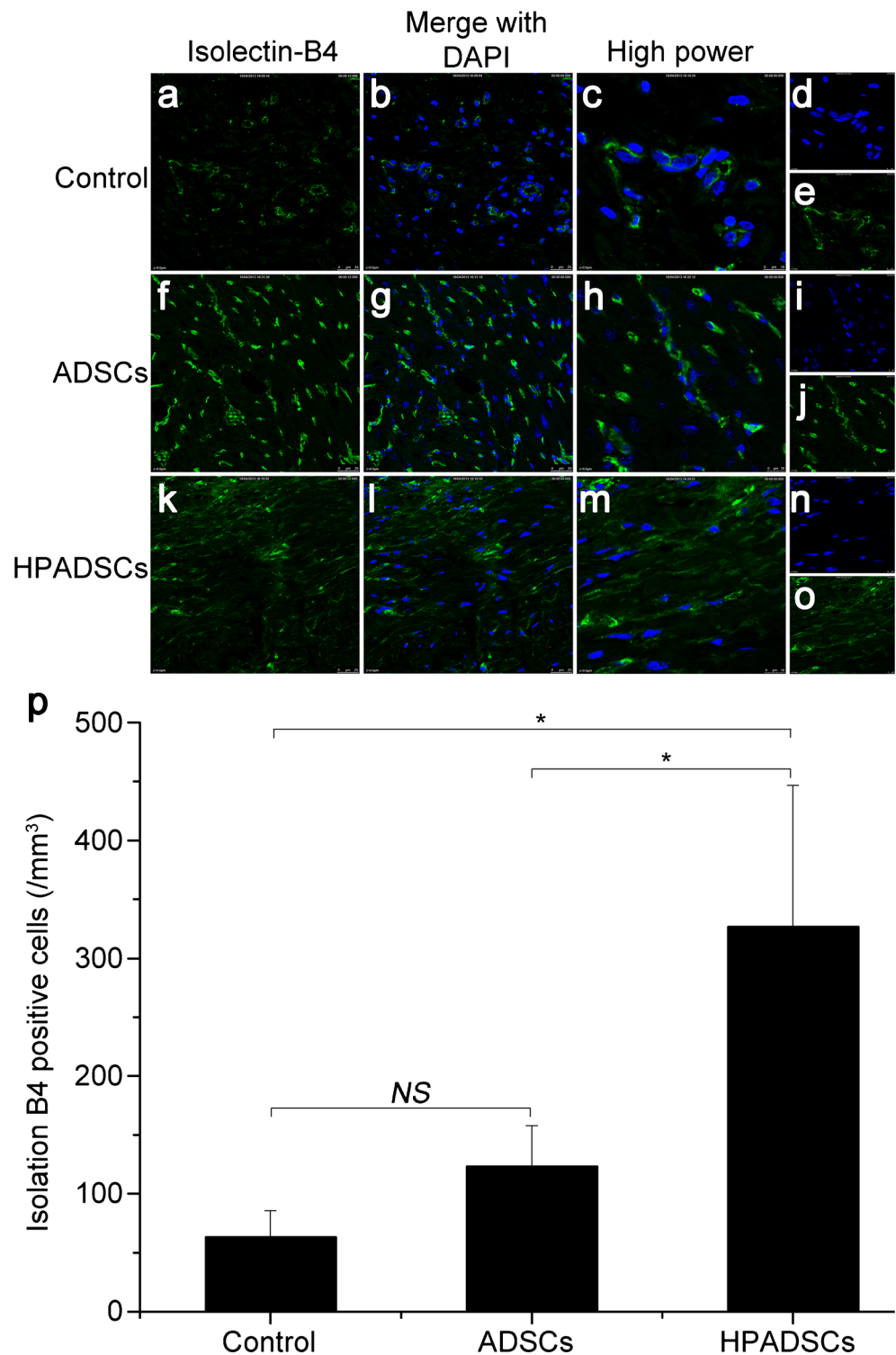


**Fig. 6** Immunohistochemistry staining with CD4 and vWF antibodies was used to quantify the number of inflammatory cells and the capillary density (a–f). CD4 staining indicated increased inflammatory cell infiltration in the HPADSC transplantation group. vWF staining showed that the increase in capillary density was significant in the HPADSC transplantation group (g, h). Bar 100  $\mu$ m

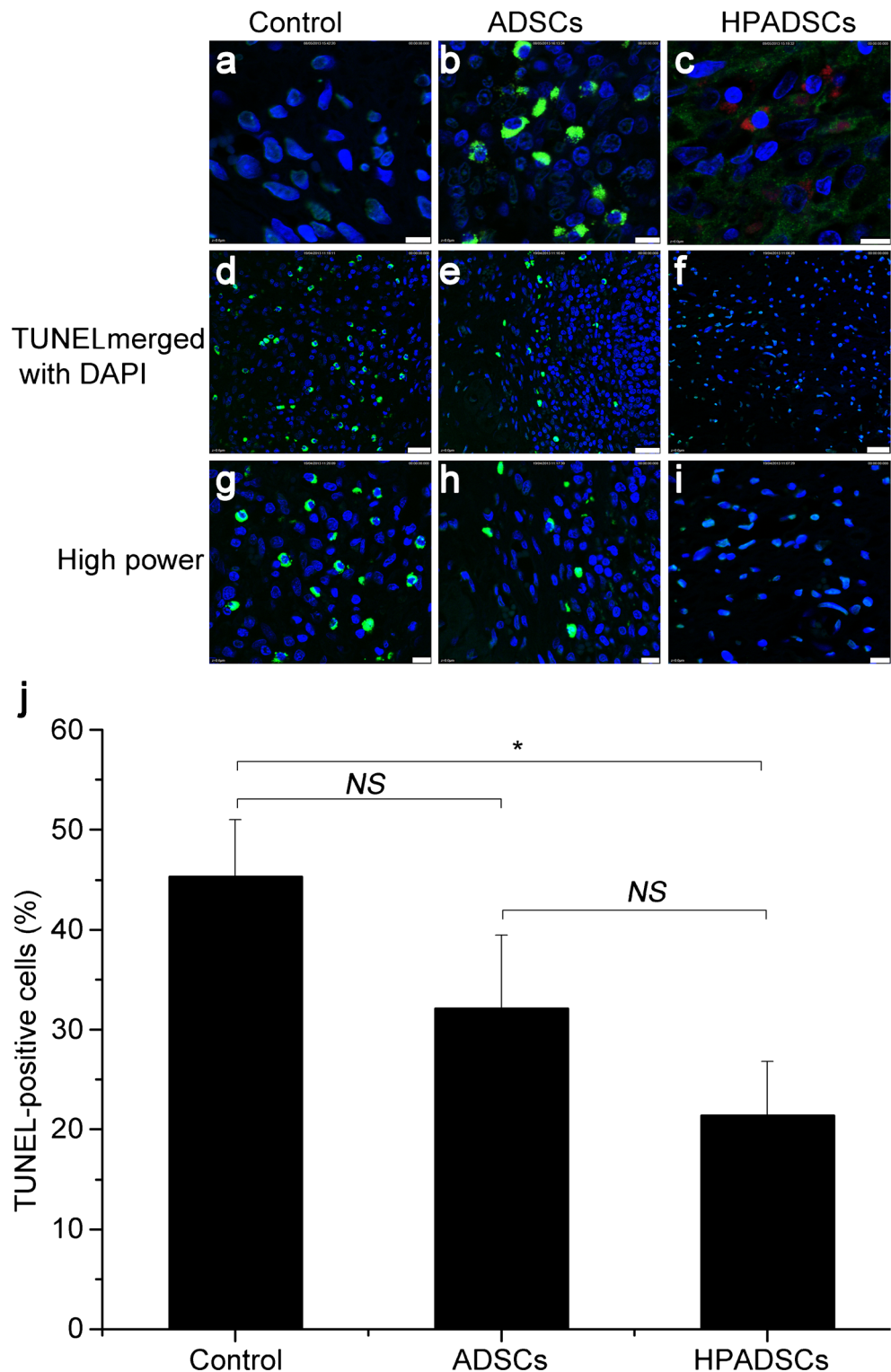
**Fig. 7** Immunofluorescent staining with an isolectin B4 (green) antibody was used to visualize the vasculature in each group (a–o). Isolectin B4 staining revealed visibly outlined vascular profiles in the peri-infarct zone (k–o). There was a considerable increase in vascular staining in the HPADSC transplantation group (p). Bar 25 μm



infarction area, we examined the newly formed blood vessels, engraftment and proliferation in the ADSC and HPADSC groups using antibodies isolectin B4, specific to human beta-2 microglobulin, and Ki67 (Figs. 7a–o, 8a–c). There were

more isolectin B4-positive cells in the HPADSC transplant group compared with the ADSC transplant group ( $326.65 \pm 120.33$  compared with  $123.18 \pm 34.67/\text{mm}^2$ ,  $P=0.044$ ) or the control group ( $326.65 \pm 120.33$  compared with  $63.17 \pm 22.38/$

**Fig. 8** Human beta-2 microglobulin (green) and Ki67 (red) antibodies were used to evaluate the engraftment and proliferation of cells in each group. Control (a). Human beta-2 microglobulin was positive in the ADSC group (b), Ki67 and human beta-2 microglobulin staining was positive in the HPADSCs group (c), indicating that the HPADSC were engaged and proliferating in the MI after 6 weeks. Bar 7.5  $\mu$ m. TUNEL fluorescence showed that the rate of cellular apoptosis decreased significantly in the HPADSC transplantation groups. TUNEL-positive cell (green) overlapped with nuclei (blue) ( $*P<0.05$ ) (d–j). Bar 25  $\mu$ m



$\text{mm}^2$ ,  $P=0.014$ ), indicating that HPADSCs could significantly promote angiogenesis (Fig. 7p). The human beta-2 microglobulin-positive cells in the ADSC transplant group showed that ADSCs could survive in the MI for up

to 6 weeks (Fig. 8b). The double positive staining of Ki67 and human beta-2 microglobulin in the HPADSC group indicated that HPADSCs could engraft and proliferate in the MI (Fig. 8c).



The TUNEL-positive nuclei in the HPADSC transplant group were significantly decreased in the myocardium of the peri-infarct zones compared with the control group ( $21.4 \pm 5.38$  compared with  $45.32 \pm 5.69$  %,  $P = 0.008$ ). There was no significant difference between the ADSC transplantation group and the control group ( $32.13 \pm 7.32$  compared with  $45.32 \pm 5.69$  %,  $P = 0.083$ ; Fig. 8d–j).

## Discussion

In the present study, we demonstrated that ADSCs secreted more cytokines after being cultured in a hypoxic environment for 24 h, and their anti-apoptotic capabilities were improved by culturing under 3 % oxygen. In addition, when the oxygen concentration was too low, the ADSCs were apoptotic. Therefore, we selected 3 % oxygen as the ideal hypoxic preconditioning condition. After the HPADSCs were transplanted, they promoted angiogenesis, reduced the level of myocardial apoptosis and the infarct size and improved the cardiac function of the AMI.

It is likely that no single factor defines the hostile micro-environment of an injured myocardium. Oxidative stress and an intense inflammatory reaction are known to prevent the homing of donor cells, thus reducing the success of cell therapies. Similarly, some degree of fibrosis is required to prevent myocardial rupture after a myocardial infarction, but dense fibrosis presents a barrier to regenerating cells (Frangogiannis et al. 2002). Therefore, many strategies have been applied to optimize and enhance the survival, activation and homing to injury sites of the transplanted cells. Preconditioning is an endogenous protective mechanism that allows cells to adapt to the environment by changing their function (Bolli 2000). To date, there have been several methods used to improve the therapeutic potential of implanted cells, such as exposure to hypoxia (Stubbs et al. 2012; Lavrentieva et al. 2010), cytokines (Pasha et al. 2008) and pharmacological treatments (Spallotta et al. 2010; Landmesser et al. 2004). Prior to transplantation, preconditioning renders cells more resistant to a harsh environment. Among these preconditioning methods, we found that hypoxia is an effective and convenient method to upregulate the transcription of growth factors that induce neoangiogenesis and neovascularization. Several reports have shown a protective role for hypoxic preconditioning in several stem cell types and have highlighted its pro-survival and pro-regenerative effects (Hu et al. 2008; Kubo et al. 2009; Tang et al. 2009). When cells encounter severe hypoxic conditions, ranging from 0.4 to 2.3 %  $O_2$ , it often results in cellular apoptosis. Conversely, a short period of exposure to mild hypoxic conditions results in cell survival in the ischemic tissue (Cencioni

et al. 2012). In previous studies, many researchers have focused on the impact of a single oxygen concentration on transplanted cells. They selected different oxygen concentrations for their culture conditions, making it difficult to compare the various studies. Although similar studies on the impact of hypoxic conditions (1.5, 2.5, and 5 %  $O_2$ ) on umbilical cord-derived human mesenchymal stem cells have been reported, these studies focused on the proliferative and metabolic activities of the cells instead of the changes in cytokine expression and cellular apoptosis (Lavrentieva et al. 2010). In our in vitro study, we used qRT-PCR and western blots to analyze cytokine secretion at the mRNA and protein levels, respectively, as well as cell survival. In addition, Matrigel morphogenesis assays indicated that the HPADSC-conditioned medium could promote the capillary-like tube formation of endothelial cells. Finally, we found that 3 % oxygen is the ideal precondition for ADSCs.

Intramyocardial injection directly into the myocardium (Bo et al. 2005; Henning et al. 2006; Yamada et al. 2007) is considered the most reliable method of delivery that results in higher cell retention within the myocardium (Dib et al. 2010; Menasche et al. 2008). The surgical exposure of the heart provides visualization of the epicardium, and therapy is administered to the external surface of the heart via a standard syringe. In the future, cell transplantation could be combined with coronary artery bypass grafts or other open heart procedures.

Usually, cell transplantation occurs hours to days after MI induction, even though the MI model is performed by ligation of LAD. Although this method is not widely used, some experimental studies on the treatment of cardiovascular disease describe the administration of the cells or stent immediately after the MI induction (Lin et al. 2010; Jammel et al. 2010; Galvez-Monton et al. 2011; Wang et al. 2009a).

Furthermore, cardiac repair after myocardial infarction can be divided into three overlapping phases: the inflammatory phase, the proliferative phase and the maturation/healing phase (Liehn et al. 2011; Frangogiannis 2006). In different phases, cell transplantation plays different roles in MI repair. Malek et al. (2006) found that the severity of the acute inflammation is critical for stem cell recruitment in a murine myocarditis model. Delivery of embryonic stem cells at the peak of inflammation (the time point with the highest cytokine production) following induction of myocarditis resulted in the highest level of stem cell engraftment in the heart and the greatest functional improvement 3 months later. In the majority of studies, stem cells have been transplanted in the proliferative phase (days after MI induction). In this phase, cardiomyocyte regeneration is an important factor. The goal of cell transplantation is to restore the initial integrity of the heart tissue (Hatzistergos et al. 2010). In the maturation/healing phase, stem cells are transplanted into the mature scar, which induces cell-specific changes and improves ventricular

function (Schuh et al. 2009). Transplantation in the mature phase could benefit patients with extended scar tissue in clinical applications.

Intramyocardial transplantation of ADSCs has been shown to benefit the infarcted myocardium (Landmesser et al. 2004). We reported similar contributions to cardiac functional improvement after ADSC implantation in swine. Furthermore, we demonstrated that HPADSC transplantation resulted in a greater improvement of cardiac function. The implanted ADSCs promote angiogenesis and prevent further apoptosis of the cardiomyocytes around the infarct zone, leading to the preservation of cardiac function (Bagno et al. 2012; Rigol et al. 2010). Our results showed more cells that stained positive for isolectin B4 and fewer apoptotic cells in the HPADSC transplantation group, which may be related to the overexpression of VEGF, HGF, PLGF and Bcl-2 in the ADSCs cultured under 3 % oxygen. Therefore, the survival and anti-apoptotic capability of the ADSCs is improved in the MI microenvironment, ultimately promoting angiogenesis and decreasing cardiomyocyte apoptosis. In fact, the HPADSC transplantation group exhibited a smaller infarct size, better regional perfusion and improved wall motion coordination based on the echocardiography and 99mTC-SPECT scans.

The mechanisms of MI therapy by ADSCs are mainly related to direct differentiation and paracrine signaling; however, the relative roles of these two mechanisms are uncertain (Gnecchi et al. 2008). The paracrine effect of stem cells is thought to be the main mechanism of MI therapy, an idea which has been gradually accepted. The paracrine products of ADSCs include various cytokines or growth factors, such as VEGF, HGF, IGF-1 and others, that can regulate cell apoptosis, angiogenesis, inflammation and the mobilization of endogenous cardiac stem cells (Mirotsoy et al. 2011; Tang et al. 2011).

The differentiation potential of transplanted ADSCs in the ischemic heart to transform into cells of the cardiac lineages is controversial. Some reports show that ADSCs possess the capacity to transdifferentiate into cardiomyocytes, endothelial cells and smooth muscle cells after transplantation into the heart (Wang et al. 2009b; Bayes-Genis et al. 2010). Although cardiomyocyte-specific markers were detected in our study (data not shown), the number of stem cells that differentiated into cardiomyocytes was small; whether these differentiated cells can function as normal cardiomyocytes remains uncertain. Similarly, Yang et al. (2013) found that ADSC differentiation is only of minor benefit for the treatment of MI, while the therapeutic benefit of ADSC transplantation is mainly induced by paracrine-mediated cardioprotection and angiogenesis.

Nevertheless, further studies are needed to address the following limitations of our study. First, we showed hypoxic preconditioning could improve the viability of ADSCs;

however, *in vivo* studies are needed to confirm the effects of hypoxic preconditioning on gene expression in stem cells. Second, we measured the therapeutic effect at a single time point and, therefore, did not evaluate other cell culture conditions or other cell transplant doses. Third, cell transplantation plays different roles during the different phases of cardiac repair. At present, the optimal timing of cell transplantation is not clear. In our study, we administered HPADSCs or ADSCs immediately to improve the engraftment, but we did not compare the therapeutic effect between cells administered immediately and cells administered some days after MI. And, fourth, because the animals received cyclosporine, the results obtained may limit the clinical applications. The potential therapeutic effects in AMI patients will have to be investigated in future clinical trials. Further studies should be designed to address all of these problems.

In conclusion, culturing hADSCs in 3 % oxygen enhanced their ability to protect against apoptosis and to secrete cytokines. After transplantation into the peri-infarct zone, the HPADSCs promoted angiogenesis, increased myocardial perfusion, reduced the infarct area, and improved cardiac function. HPADSC transplantation may be an effective method for the treatment of AMI in clinical applications.

**Acknowledgments** This work was supported by Tianjin Binhai New Area Health Bureau projects (Grants: 2012BWKZ009), the State High-tech Research and Development Plan (Grants: 2011AA020109) and China National Natural Science Foundation (Grants: 81301217). Alliances Bioscience Co. Ltd. is also gratefully acknowledged for assistance with ADSC.

**Conflict of interest** None

## References

- Bagno LL, Wernick-de-Castro JP, Oliveira PF, Cunha-Abreu MS, Rocha NN, Kasai-Brunswick TH, Lago VM, Goldenberg RC, Campos-de-Carvalho AC (2012) Adipose-derived stromal cell therapy improves cardiac function after coronary occlusion in rats. *Cell Transplant* 21: 1985–1996
- Bayes-Genis A, Soler-Botija C, Farre J, Sepulveda P, Raya A, Roura S, Prat-Vidal C, Galvez-Monton C, Montero JA, Buscher D, Izpisua Belmonte JC (2010) Human progenitor cells derived from cardiac adipose tissue ameliorate myocardial infarction in rodents. *J Mol Cell Cardiol* 49:771–780
- Bo K, Tian H, Prasongsukarn K, Wu J, Anquoultant D, Wnendt S, Muhs A, Spitzkovsky D, Li RK (2005) Cell transplantation improves ventricular function after a myocardial infarction: a preclinical study of human unrestricted somatic stem cells in a porcine model. *Circulation* 112(9 Suppl):I95–I104
- Bolli R (2000) The late phase of preconditioning. *Circ Res* 87:972–983
- Cencioni C, Capogrossi MC, Napolitano M (2012) The SDF-1/CXCR4 axis in stem cell preconditioning. *Cardiovasc Res* 94:400–407
- Dib N, Menasche P, Bartunek JJ, Zeiher AM, Terzic A, Chronos NA, Henry TD, Peters NS, Fernandez-Aviles F, Yacoub M, Sanborn TA, Demaria A, Schatz RA, Taylor DA, Fuchs S, Itescu S, Miller LW, Dinsmore JH, Danqas GD, Popma JJ, Hall JL, Holmes DR Jr (2010)

- Recommendations for successful training on methods of delivery of biologics for cardiac regeneration: a report of the international society for cardiovascular translational research. *J Am Coll Cardiol Intv* 3:265–275
- Efimenko A, Starostina E, Kalinina N et al (2011) Angiogenic properties of aged adipose derived mesenchymal stem cells after hypoxic conditioning. *J Transl Med* 9:10
- Fraccarollo D, Galuppo P, Bauersachs J (2012) Novel therapeutic approaches to post-infarction remodeling. *Cardiovasc Res* 94:293–303
- Frangogiannis NG (2006) The mechanistic basis of infarct healing. *Antioxid Redox Signal* 8:1907–1939
- Frangogiannis NG, Smith CW, Entman ML (2002) The inflammatory response in myocardial infarction. *Cardiovasc Res* 53:31–47
- Freyman T, Polin G, Osman H, Crary J, Lu M, Cheng L, Palasis M, Wilensky RL (2006) A quantitative, randomized study evaluating three methods of mesenchymal stem cell delivery following myocardial infarction. *Eur Heart J* 27:1114–1122
- Fuchs S, Baffour R, Zhou YF, Shou M, Pierre A, Tio FO, Weissman NJ, Leon MB, Epstein SE, Komowski R (2001) Transendocardial delivery of autologous bone marrow enhances collateral perfusion and regional function in swines with chronic experimental myocardial ischemia. *J Am Coll Cardiol* 37:1726–1732
- Galvez-Monton C, Prat-Vidal C, Roura S, Farre J, Soler-Botija C, Lucia-Valldeperas A, Diaz-Guemes I, Sanchez-Margallo FM, Aris A, Bayes-Genis A (2011) Transposition of a pericardial-derived vascular adipose flap for myocardial salvage after infarct. *Cardiovasc Res* 91:659–667
- Gnecchi M, Zhang Z, Ni A, Dzau VJ (2008) Paracrine mechanisms in adult stem cell signaling and therapy. *Circ Res* 103:1204–1219
- Hatzistergos KE, Quevedo H, Oskouei BN, Hu Q, Feigenbaum GS, Margitich IS, Mazhari R, Boyle AJ, Zambrano JP, Rodriguez JE, Dulce R, Pattany PM, Valdes D, Revilla C, Heldman AW, McNiece I, Hare JM (2010) Bone marrow mesenchymal stem cells stimulate cardiac stem cell proliferation and differentiation. *Circ Res* 107:913–922
- Henning RJ, Burgos JD, Ondrovic L, Sanberg P, Balis J, Morqan MB (2006) Human umbilical cord blood progenitor cells are attracted to infarcted myocardium and significantly reduce myocardial infarction size. *Cell Transplant* 15:647–658
- Houtgraaf JH, den Dekker WK, van Dalen BM, Springeling T, de Jong R, van Geuns RJ, Geleijnse ML, Fernandez-Aviles F, Zijlstra F, Serruys PW, Duckers HJ (2012) First experience in humans using adipose tissue-derived regenerative cells in the treatment of patients with ST-segment elevation myocardial infarction. *J Am Coll Cardiol* 59:539–540
- Hu X, Yu SP, Fraser JL, Lu Z, Ogle ME, Wang JA, Wei L (2008) Transplantation of hypoxia-preconditioned mesenchymal stem cells improves infarcted heart function via enhanced survival of implanted cells and angiogenesis. *J Thorac Cardiovasc Surg* 135:799–808
- Jammel MN, Li Q, Mansoor A, Qiang X, Sarver A, Wang X, Swingen C, Zhang J (2010) Long term functional improvement and gene expression changes after bone marrow-derived multipotent progenitor cell transplantation in myocardial infarction. *Am J Physiol Heart Circ Physiol* 298:H1348–H1356
- Kim B-O, Tian H, Prasongsukarn K, Jun W, Angoulvant D, Wnendt S, Muhs A, Spitkovsky D, Li R-K (2005) Cell Transplantation Improves Ventricular Function After a Myocardial Infarction: A Preclinical Study of Human Unrestricted Somatic Stem Cells in a Porcine Model. *Circulation* 112:1096–1104
- Kim JH, Park SH, Park SG, Choi JS, Xia J, Sung JH (2011) The pivotal role of reactive oxygen species generation in the hypoxia-induced stimulation of adipose-derived stem cells. *Stem Cells Dev* 20:1753–1761
- Kim JH, Song SY, Park SG, Song SU, Xia Y, Sung JH (2012) Primary involvement of NADPH oxidase 4 in hypoxia-induced generation of reactive oxygen species in adipose-derived stem cells. *Stem Cell Dev* 21:2212–2221
- Kubo M, Li TS, Kamota T, Ohshima M, Qin SL, Hamano K (2009) Increased expression of CXCR4 and integrin alphaM in hypoxia-preconditioned cells contributes to improved cell retention and angiogenic potency. *J Cell Physiol* 220:508–514
- Landmesser U, Engberding N, Bahlmann FH, Schaefer A, Wiencke A, Heineke A, Spiekermann S, Hilfiker-Kleiner D, Templin C, Kotlarz D, Mueller M, Fuchs M, Homig B, Haller H, Drexler H (2004) Statin-induced improvement of endothelial progenitor cell mobilization, myocardial neovascularization, left ventricular function, and survival after experimental myocardial infarction requires endothelial nitric oxide synthase. *Circulation* 110:1933–1939
- Lavrentieva A, Majore I, Kasper C, Hass R (2010) Effects of hypoxic culture conditions on umbilical cord-derived human mesenchymal stem cells. *Cell Commun Signal* 8:18
- Liehn EA, Postea O, Curai A, Marx N (2011) Repair after myocardial infarction, between fantasy and reality. *J Am Coll Cardiol* 58:2357–2362
- Lin YD, Yeh ML, Yang YJ, Tsai DC, Chu TY, Shih YY, Chang MY, Liu YW, Tang AC, Chen TY, Luo CY, Chang KC, Chen JH, Wu HL, Hung TK, Hsieh PC (2010) Intramyocardial peptide nanofiber injection improves postinfarction ventricular remodeling and efficacy of bone marrow cell therapy in pigs. *Circulation* 122:S132–S141
- Lopez AD, Mathers CD, Ezzati M, Jamison DT, Murray CJ (2006) Global and regional burden of disease and risk factors, 2001: systematic analysis of population health data. *Lancet* 367:1747–1757
- Malek S, Kaplan E, Wang JF, Ke Q, Rana JS, Chen Y, Rahim BG, Li M, Huang Q, Xiao YF, Verheugt FW, Morgan JP, Min JY (2006) Successful implantation of intravenously administered stem cells correlates with severity of inflammation in murine myocarditis. *Pflugers Arch* 452:268–275
- Mazo M, Gavira JJ, Pelacho B, Prosper F (2011) Adipose-derived stem cells for myocardial infarction. *J Cardiovasc Transl Res* 4:145–153
- Menasche P, Alifrieri O, Janssens S, McKenna W, Reichenspurner H, Trinquart L, Marolleau JP, Vilquin JT, Seymour B, Larqhero J, Lake S, Chatellier G, Solomon S, Desnos M, Hagege AA (2008) The myoblast autologous grafting in ischemic cardiomyopathy (MAGIC) trial: first randomized placebo-controlled study of myoblast transplantation. *Circulation* 117:1190–1191
- Mirotsov M, Jayawardena TM, Schmeckpeper J, Gnecchi M, Dzau VJ (2011) Paracrine mechanisms of stem cell reparative and regenerative actions in the heart. *J Mol Cell Cardiol* 50:280–289
- Panfilov IA, de Jong R, Takashima S, Duckers HJ (2013) Clinical study using adipose-derived mesenchymal-like stem cells in acute myocardial infarction and heart failure. *Methods Mol Biol* 1036:207–212
- Pasha Z, Wang Y, Sheikh R, Zhang D, Zhao T, Ashraf M (2008) Preconditioning enhances cell survival and differentiation of stem cells during transplantation in infarcted myocardium. *Cardiovasc Res* 77:134–142
- Qu X, Liu T, Song K, Li X, Ge D (2013) Induced Pluripotent Stem Cells Generated from Human Adipose-Derived Stem Cells Using a Non-Viral Polycistronic Plasmid in Feeder-Free Conditions. *PLoS ONE* 7:e48161
- Reddy KS (2004) Cardiovascular disease in non-western countries. *N Engl J Med* 350:2438–2440
- Rigol M, Solanes N, Farre J, Roura S, Roque M, Berrueto A, Bellera N, Novensa L, Tamborero D, Prat-Vidal C, Huzman MA, Battle M, Hoefsloot M, Sitges M, Ramirez J, Dantas AP, Merino A, Sanz G, Brugada J, Bayes-Genis A, Heras M (2010) Effects of adipose tissue-derived stem cell therapy after myocardial infarction: impact of the route of administration. *J Card Fail* 16:357–366
- Schuh A, Liehn EA, Sasse A, Schneider R, Neuss S, Weber C, Kelm M, Merx MW (2009) Improved left ventricular function after

- transplantation of microspheres and fibroblasts in a rat model of myocardial infarction. *Basic Res Cardiol* 104:403–411
- Spallotta F, Rosati J, Straino S, Nanni S, Grasselli A, Ambrosino V, Rotili D, Valente S, Farsetti A, Mai A, Capogrossi MC, Gaetano C, Illi B (2010) Nitric oxide determines mesodermic differentiation of mouse embryonic stem cells by activating class IIa histone deacetylases: potential therapeutic implications in a mouse model of hindlimb ischemia. *Stem Cells* 28:431–442
- Stubbs SL, Hsiao ST, Peshavariya HM, Lim SY, Disting GJ, Dilley RJ (2012) Hypoxic preconditioning enhances survival of human adipose-derived stem cells and conditions endothelial cells in vitro. *Stem Cells Dev* 21:1887–1896
- Tang YL, Zhu W, Cheng M, Chen L, Zhang J, Sun T, Kishore R, Phillips MI, Losordo DW, Qin G (2009) Hypoxic preconditioning enhances the benefit of cardiac progenitor cell therapy for treatment of myocardial infarction by inducing CXCR4 expression. *Circ Res* 104:1209–1216
- Tang JM, Wang JN, Zhang L, Zheng F, Yang JY, Kong X, Guo LY, Chen L, Huang YZ, Wan Y, Chen SY (2011) VEGF/SDF-1 promotes cardiac stem cell mobilization and myocardial repair in the infarcted heart. *Cardiovasc Res* 91:402–411
- Wang Y, Liu XC, Zhang GW, Zhao J, Zhang JM, Shi RF, Huang YZ, Zhao CH, Liu TJ, Song CX, Lu F, Yang Q, He GW (2009a) A new transmyocardial degradable stent combined with growth factor, heparin, and stem cells in acute myocardial infarction. *Cardiovasc Res* 84:461–469
- Wang L, Deng J, Tian W, Xiang B, Yang T, Li G, Wang J, Gruwel M, Kashour T, Rendell J, Glogowski M, Tomanek B, Freed D, Deslauriers R, Arora RC, Tian G (2009b) Adipose-derived stem cells are an effective cell candidate for treatment of heart failure: an MR imaging study of rat hearts. *Am J Physiol Heart Circ Physiol* 297:H1020–H1031
- Yamada Y, Yokoyama S, Fukuda N, Kidoya H, Huang XY, Naitoh H, Satoh N, Takakura N (2007) A novel approach for myocardial regeneration with educated cord blood cells cocultured with cells from brown adipose tissue. *Biochem Biophys Res Commun* 353:182–188
- Yang D, Wang W, Li L, Peng Y, Chen P, Huang H, Guo Y, Xia X, Wang Y, Wang H, Wang WE, Zeng C (2013) The relative contribution of paracrine effect versus direct differentiation on adipose-derived stem cell transplantation mediated cardiac repair. *PLoS ONE* 8:e59020